Mechanisms of Action of Mixed Solid−Liquid Antifoams. 1. Dynamics of Foam Film Rupture

Nikolai D. Denkov,* Philip Cooper, and Jean-Yves Martin

Usine Silicones, RHODIA Chimie, CRIT C, 55 Rue des Freres Perret BP 22, 69191 Saint Fons Cedex, France

Received February 23, 1999. In Final Form: May 5, 1999

Antifoams (usually consisting of a mixture of hydrophobic solid particles and oils) are widely used in different technological applications to prevent the formation of excessive foam. Uncertainty still exists in the literature about the actual mechanisms by which these substances destroy the foam. To elucidate this problem, we have performed microscopic observations on the process of foam film destruction by means of a high-speed camera. Horizontal and vertical foam films (obtained from solutions of the surfactant sodium dioctyl sulfosuccinate) were studied in the presence of antifoam particles containing silicone oil and hydrophobized silica. The observations show that in this system the antifoam particles destroy the foam lamella by the formation of unstable oil bridges, which afterward stretch and eventually rupture, due to uncompensated capillary pressures across the different interfaces. These bridges can be formed either from initially emulsified antifoam droplets, which enter both surfaces of the foam film during its formation and thinning, or from oil lenses which float on the bulk air−water interface even before the foam film is formed. We show that the presence of an oil layer having a thickness of several nanometers, prespread over the foam film surfaces, is very important for the process of lamella destruction, because this layer substantially facilitates the entry of the oil drops on the film surface and the formation of unstable bridges. The process of oil-bridge stretching, which is usually not considered in the standard mechanisms of antifoam action, is theoretically analyzed in the second part of this study.

Introduction

Antifoams are widely used in different technologies, such as paper production, textile dyeing, drug manufacturing, and throughout the oil industry, to reduce the volume of unwanted foam.[1] Antifoams are important additives for various commercial products, like detergents, paints, pharmaceuticals, and others.[1] A typical antifoam can consist of a hydrophobic oil (possibly preemulsified), dispersed hydrophobic solid particles, or a mixture of both.[2,3]

The role of the oil (hydrocarbon or poly(dimethylsiloxane)) in liquid or in mixed solid−liquid antifoams is usually explained in the framework of two mechanisms of foam film destruction: (i) spreading-fluid entrainment[4−10] and (ii) bridging-dewetting.[2,8−14] According to the spreading mechanism, the effective antifoam contains oil that spreads rapidly over the foam film surface. The oil spreading leads to a Marangoni-driven flow of liquid in the foam film (fluid entrainment), resulting in a local film thinning and subsequent rupture—see Figure 1. For the bridging mechanism, oil drop penetration through both film surfaces is implied, creating an oil "bridge" between them. The hydrophobic surface of the oil induces a dewetting of the bridge and a subsequent film rupture (Figure 1). As discussed by Bergeron et al.,[10] these two mechanisms do not necessarily exclude each other—a spreading of the oil could facilitate the bridging by reducing the local film thickness. On the basis of the above concepts and following the original works of Robinson and Woods[15] and Ross,[4] the antifoam efficiency is often estimated in terms of the so-called entry coefficient E and spreading coefficient S, defined as

$$E = \sigma_{AW} + \sigma_{OW} - \sigma_{OA} \quad (1)$$

$$S = \sigma_{AW} - \sigma_{OW} - \sigma_{OA} \quad (2)$$

where σ are interfacial tensions and the subscripts AW, OW, and OA refer to air−water, oil−water, and oil-air interfaces, respectively. Positive values of E and S are considered to correspond to easy entry and spreading of the oil drop, respectively, and lead to high antifoam efficiency. One should distinguish between the initial values of E and S (calculated from the interfacial tensions of nonequilibrated antifoam and surfactant solution) and their final values (after equilibration of the phases), which might even have different signs.[2] For example, the initial

* To whom correspondence should be addressed. Permanent address: Laboratory of Thermodynamics and Physicochemical Hydrodynamics, Faculty of Chemistry, Sofia University, 1 James Bourchier Ave., 1126 Sofia, Bulgaria. Phone: (+359) 2-962 5310. Fax: (+359) 2-962 5643. E-mail: ND@LTPH.BOL.BG.

(1) *Defoaming: Theory and Industrial Applications*; Garrett, P. R., Ed.; Marcel Dekker: New York, 1993; Chapters 2−8.
(2) Garrett, P. R. In *Defoaming: Theory and Industrial Applications*; Garrett, P. R., Ed.; Marcel Dekker: New York, 1993; Chapter 1.
(3) Pugh, R. J. *Adv. Colloid Interface Sci.* **1996**, *64*, 67.
(4) Ross, S. *J. Phys. Colloid Chem.* **1950**, *54*, 429.
(5) Ewers, W. E.; Sutherland, K. L. *Aust. J. Sci. Res.* **1952**, *5*, 697.
(6) Shearer, L. T.; Akers, W. W. *J. Phys. Chem.* **1958**, *62*, 1264, 1269.
(7) Prins, A. In *Food Emulsions and Foams*; Dickinson, E., Ed.; Royal Society of Chemistry Special Publication, Vol. 58; Royal Society of Chemistry: Letchworth, U.K., 1986; p 30.
(8) Aveyard, R.; Binks, B. P.; Fletcher, P. D. I.; Peck, T.-G.; Garrett, P. R. *J. Chem. Soc., Faraday Trans.* **1993**, *89*, 4313.
(9) Aveyard, R.; Binks, B. P.; Fletcher, P. D. I.; Peck, T. G.; Rutherford, C. E. *Adv. Colloid Interface Sci.* **1994**, *48*, 93.
(10) Bergeron, V.; Cooper, P.; Fischer, C.; Giermanska-Kahn, J.; Langevin, D.; Pouchelon, A. *Colloids Surf., A: Physicochem. Eng. Aspects* **1997**, *122*, 103.
(11) Garrett, P. R.; Moor, P. R. *J. Colloid Interface Sci.* **1993**, *159*, 214.
(12) Garrett, P. R.; Davis, J.; Rendall, H. M. *Colloids Surf., A: Physicochem. Eng. Aspects* **1994**, *85*, 159.
(13) Koczo, K.; Koczone, J. K.; Wasan, D. T. *J. Colloid Interface Sci.* **1994**, *166*, 225.
(14) Aveyard, R.; Cooper, P.; Fletcher, P. D. I.; Rutherford, C. E. *Langmuir* **1993**, *9*, 604.
(15) Robinson, J. V.; Woods, W. W. *J. Soc. Chem. Ind.* **1948**, *67*, 361.

10.1021/la9902136 CCC: $18.00 © 1999 American Chemical Society
Published on Web 11/23/1999

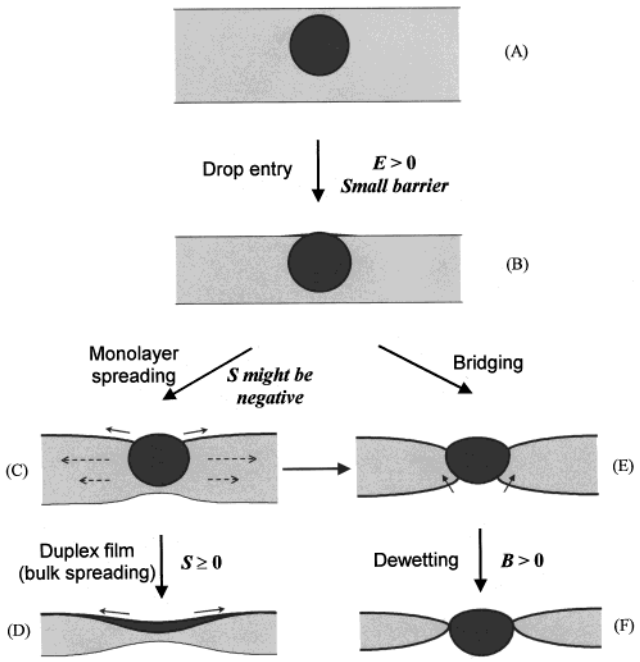

Figure 1. Two possible mechanisms of foam film rupture by antifoam particles, which are usually discussed in the literature:[2] spreading-fluid entrainment and bridging−dewetting. In both mechanisms the first step is the particle entry (A → B), which requires both a positive entry coefficient E and a small force barrier that could prevent the thinning of the oil−water−air film. The spreading of the oil over the foam film surface leads to Marangoni-driven flow of water radially from the oil drop, resulting in a local film thinning and rupture (B → C → D). Alternatively, the formation of an oil bridge between the two film surfaces could lead to dewetting of the hydrophobic antifoam particle, with subsequent rupture of the foam lamella (B → E → F). Our experiments suggest another mechanism of foam film destruction—see Figure 11.

value of S might be positive, negative, or zero, while the final (equilibrium) value might be either negative or zero.[8,16]

The critical analysis of the available experimental data made by Garrett[2] has shown that positive values of E indeed appear to be a necessary condition for having an effective antifoam, in the sense that negative values of E definitely mean poor (if any) antifoam performance. However, positive values of E do not necessarily guarantee high performance, which means that other factors might be of critical importance as well. On the other side, the analysis[2] of the available experimental data has shown that there is no straightforward correlation between the values of S and the antifoam efficiency. Moreover, in a recent study Garrett et al.[12] unambiguously showed that the oil spreading is not a necessary condition for having antifoam activity (although it might be helpful, as we will see below). Further discussion about the values of E and S and their importance for the antifoam action is presented in the Discussion section.

As shown by Garrett,[17] the stability of the oil bridges can be quantified in terms of another quantity called the bridging coefficient B. The theoretical analysis predicts that positive values of B correspond to unstable bridges and vice versa. The definition of B, as well as a further development of the model suggested by Garrett, is presented and discussed in detail in the subsequent, second part of this study.[18]

The main advantage of the above approach is that the values of E, S, and B can be determined by measuring the respective interfacial tensions. However, it does not account explicitly for the barrier against rupture of the asymmetrical oil−water−air film, which appears when the oil drop approaches the foam film surface[19−22] (Figure 1). This barrier is created by the surface forces (electrostatic, van der Waals, etc.) and by the hydrodynamic friction in the thinning oil−water−air film. This is probably one of the major reasons for the absence of a good correlation between antifoam efficiency and the values of E, S, and B. As a result, the values of E, S, and B can be used in practice only as a preliminary screening criterion to help in selecting a particular oil for a given surfactant system.

The importance of the barrier against drop entry was explored in some recent studies.[19,22,23] Lobo and Wasan[22] suggested to use the energy of interaction (per unit area) in the oil−water−air film f as a quantitative criterion of its stability:

$$f = -\int_{h\to\infty}^{h_E} \Pi \, dh \tag{3}$$

In a parallel study, Bergeron et al.[23] suggested the so-called generalized entry coefficient

$$E_g = -\int_{\Pi(h\to\infty)=0}^{\Pi(h_E)} h \, d\Pi \tag{4}$$

$\Pi(h)$ in eqs 3 and 4 denotes the disjoining pressure, while h_E is the equilibrium thickness of the oil−water−air film. As shown by Bergeron et al.,[23] the classical entry coefficient (eq 1) can be obtained as a particular case of E_g by a proper choice of the integration limit in eq 3, namely $h_E \to 0$.

The above definitions (eqs 3 and 4) are conceptually significant, because they stress the importance of the barrier which can prevent particle entry, thus explaining why positive values of the classical coefficient E do not necessarily correspond to easy entry. Systematic comparison of the values of f and E_g with the efficiencies of practical antifoams is still missing, as there is at present no general approach to calculate the disjoining pressure isotherms $\Pi(h)$ for most practical systems, especially when solid particles are present.[24] The experimental determination of the entry barrier is also a nontrivial task.[10]

It is widely accepted[2,10−13,25,26] that the main role of the solid particles in the mixed antifoams is to destabilize the oil−water−air film, thus facilitating the drop entry (pin effect). The subsequent oil spreading or bridging is believed to lead to a rapid rupture of the aqueous film. As a result of this synergistic effect, the mixed solid−liquid formulations have typically much higher efficiency than the individual components (oil or solid particles) taken separately.[2,12] This idea found a direct confirmation in the experiments of Bergeron et al.,[10] who observed the thinning of the oil−water−air film, formed when a

(16) Rowlinson, J. S.; Widom, B. *Molecular Theory of Capillarity*; Oxford University Press: Oxford, 1989; Chapter 8.
(17) Garrett, P. R. *J. Colloid Interface Sci.* **1980**, *76*, 587.
(18) Denkov, N. D. *Langmuir* **1999**, *15*, 8530.
(19) Kulkarni, R. D.; Goddard, E. D.; Kanner, B. *J. Colloid Interface Sci.* **1977**, *59*, 468.
(20) Wasan, D. T.; Nikolov, A. D.; Huang, D. D. W.; Edwards, D. A. In *Surfactant Based Mobility Control*; Smith, D. H., Ed.; ACS Symposium Series Vol. 373; American Chemical Society: Washington, DC, 1988; p 136.
(21) Koczo, K.; Lobo, L. A.; Wasan, D. T. *J. Colloid Interface Sci.* **1992**, *150*, 492.
(22) Lobo, L.; Wasan, D. T. *Langmuir* **1993**, *9*, 1668.
(23) Bergeron, V.; Fagan, M. E.; Radke, C. J. *Langmuir* **1993**, *9*, 1704.
(24) Denkov, N. D.; Kralchevsky, P. A.; Ivanov, I. B.; Wasan, D. T. *J. Colloid Interface Sci.* **1992**, *150*, 389.

relatively large drop of silicone oil (attached to the tip of a glass capillary) approaches the surface of the surfactant solution. The experiments demonstrated a substantial barrier preventing the drop entry when the oil drop contained no solid particles (although the value of E was positive), while this barrier was significantly reduced when mixed antifoam compounds were studied. The respective mechanistic explanation in terms of the three-phase contact angles of the solid particle with the oil−water and air−water interfaces was given by Garrett.[2] Another likely role of the solid particles is to increase the penetration depth of the oil lenses, floating on the film surfaces, which in turn facilitates oil bridge formation.[13,27]

Along with the two mechanisms mentioned above (which have been more or less generally accepted in the literature), there are several other mechanisms suggested in the literature.[27−29] A comprehensive analytical review on this subject can be found in ref 2. Still, however, numerous questions related to the mechanism of antifoam action lack definite answers. First, there is no oil-containing antifoam system for which the mechanism of foam destruction has been unambiguously resolved (to the best of our knowledge). This is an important practical question, because the different mechanisms suggest different ways for improving the antifoam performance. For example, the mechanism of spreading-fluid entrainment requires an easy and fast spreading of the oil at least as a thin molecular layer (without any apparent requirement for the three-phase contact angle oil−water−air in the system), while the bridging−dewetting mechanism stresses the necessity of an appropriate three-phase contact angle (without any requirement for spreading of the oil). Furthermore, from the original paper by Garrett,[17] where the stability of oil bridges was theoretically studied, one can deduce another mechanism of bridge rupture. Instead of bridge dewetting (which is usually discussed in the literature), one can envisage a process of bridge stretching due to noncompensated capillary pressures at the oil−water and air−water interfaces, with eventual perforation of the film lamella in the center of the oil bridge. Such a possibility directly follows from the analysis of Garrett,[17] but this idea has not been developed further.

Another important unclear point is which of the structural elements (foam film or the Gibbs−Plateau border) is actually destroyed by the antifoam particles. Most of the researchers consider that the foam films are being ruptured by the antifoam (because the films rapidly thin down to thickness around 1 μm and less), while Koczo et al.[13] suggested that in static foams the antifoam particles (emulsified droplets or lenses) first escape from the foam films into the neighboring Gibbs−Plateau borders (GPBs) and get trapped there. Only afterward are the antifoam particles compressed within the thinning GPBs, which are finally destroyed. The question about the actual structural element that is destroyed by the antifoam is also very important from a practical viewpoint, because the GPBs are much larger in size (cross-section of tens to hundreds of micrometers) compared to the film thickness. Therefore, when the optimal size of the antifoam particles is estimated to correspond to the characteristic size of the destroyed structural element (film or GPB), the result is quite different in these two cases. In fact, some studies[10] suggested that it is better to have larger antifoam particles which rupture the structural elements at earlier stages of film and GPB drainage, while other studies[12,30] suggested that it is beneficial to have smaller antifoam particles because their number concentration is higher (at given weight concentration of the antifoam). Closely related is another problem concerning the mechanism of antifoam deactivation[10,31,32] (exhaustion), which is explained in the literature with a reduction of the size of the antifoam particles[10] or with an emulsification of the spread oil layer.[31]

In the present study we use several complementary experimental methods to observe the process of foam film destruction and to clarify as much as possible the actual mechanism involved in this process. The key tool in our study is a high-speed video camera, combined with microinterferometric techniques which allow changes in the foam film thickness at a very high time resolution to be monitored (on the order of 1 ms). In this way some of the processes leading to foam film rupture can be directly observed and analyzed. The results show that, in our experimental system, the antifoam particles (emulsion droplets or lenses) first bridge the surfaces of the foam film with subsequent stretching and rupture of the formed oil bridge ("bridging−stretching" mechanism). Furthermore, the importance of the prespread oil layer on the foam film surfaces emerged from the experiments, which differ from the conventional spreading-fluid entrainment concept. The obtained results provide a clear picture of the stages of the foam film destruction and suggest ideas about the key factors that could be optimized to improve the antifoam performance. The results obtained so far do not exclude the possibility that in other experimental systems (antifoam−surfactant combinations) the mechanisms of antifoam action could be different, including those from Figure 1. A larger set of experiments with different systems is required before a conclusion can be drawn about the key factors, which determine the actual mechanism in a given particular system.

Experimental Section

Materials. As a surfactant we have used sodium dioctyl sulfosuccinate ($C_{20}H_{37}O_7SNa$), which was purchased from Sigma (catalog no. D-0885) and was used as received. For brevity, hereafter, we will denote this surfactant as AOT. The surfactant concentration in the working solutions was always 10 mM, which is about 3.5 times the critical micellar concentration (cmc = 2.8 mM). All solutions were prepared with bidistilled water.

Two antifoam substances were studied: (a) Mixture of poly(dimethylsiloxane) (PDMS) oil and hydrophobized silica particles of pyrogenic origin (4.2 wt %). The silicone oil is produced by Rhodia Silicones under the commercial name 47V1000 and has a viscosity of 1000 mPa·s. Electron micrographs showed that the silica particles form aggregates in the silicone oil with a fractal structure and a rather broad size distribution (0.1−5 μm). Hereafter, this composition is labeled as compound A.

(b) Stable 10 wt % stock emulsion of compound A, which was further diluted in the surfactant solution to the desired final concentration. The stock emulsion was stabilized by two nonionic surfactants (sorbitan monostearate—Span 60 and an ethoxylate of stearic acid with 40 ethoxy groups—stearyl-EO_{40}). Microscope observations showed that this emulsion was relatively polydisperse with drop diameters ranging from 1 to 10 μm. Dynamic light scattering measurements of diluted samples provided an average number diameter of 1 μm and a mass diameter of 4.5 μm. This emulsion is denoted hereafter as emulsion A.

(25) Aronson, M. *Langmuir* **1986**, *2*, 653.
(26) Aveyard, R.; Clint, J. H. *J. Chem. Soc., Faraday Trans.* **1995**, *91*, 2681.
(27) Frye, G. C.; Berg, J. C. *J. Colloid Interface Sci.* **1989**, *130*, 54.
(28) Kulkarni, R. D.; Goddard, E. D.; Kanner, B. *Ind. Eng. Chem. Fundam.* **1977**, *16*, 472.
(29) Dippenaar, A. *Int. J. Miner. Process.* **1982**, *9*, 1.
(30) Garrett, P. R. *Langmuir* **1995**, *11*, 3576.
(31) Racz, G.; Koczo, K.; Wasan, D. T. *J. Colloid Interface Sci.* **1996**, *181*, 124.
(32) Pouchelon, A.; Araud, A. *J. Dispersion Sci. Technol.* **1993**, *14*, 447.

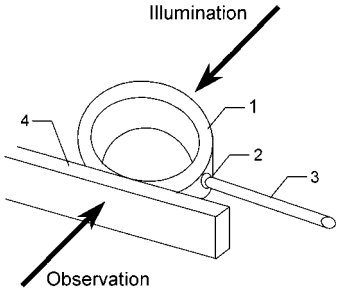

Figure 2. Schematic presentation of the Dippenaar cell.[29] A foam lamella (not shown in the figure) is formed between two concave menisci in a short capillary (1); the thickness of the foam lamella is controlled by sucking liquid through a side orifice (2); a needle (3) attached to syringe driven by a micrometric screw (not shown) is used for liquid suction; the shapes of the menisci and of the oil bridge are observed in transmitted white light; an optical glass plate (4) is used to avoid the cylindrical aberration created by the curvature of the capillary wall. The cell is closed in a container (not shown) to reduce the air convection and water evaporation.

Both antifoam compositions (compound A and emulsion A) were chosen to mimic closely commercial silicone-based antifoams. In most of the experiments the concentration of the antifoam in the working solutions was 0.01 vol %, which falls in the typical concentration range for silicone antifoams. A lower antifoam concentration (0.0012 vol %) was used in only two series of experiments with vertical foam films to study the concentration effect on the film lifetime and on the position of film rupture.

Typically, 0.1 mL of emulsion A was added to 100 mL of the AOT solution and the system was homogenized by shaking vigorously by hand five times. Since the antifoam is predispersed in the form of emulsion droplets when producing emulsion A, these five shakes were enough to homogenize the working solution. The foam produced after these shakes disappeared in about 10 s, which shows that emulsion A was a rather active antifoam under these conditions.

To disperse in a reproducible way compound A in the surfactant solutions, we needed a more refined procedure: 0.01 mL of compound A was added to 100 mL of the AOT solution in a 250 mL glass bottle, and this mixture was mechanically agitated for five cycles on a "Shake-Test" machine (Oscill 8, PROLABO). Each cycle consisted of 42 shakes of the sample for 10 s, followed by a rest period of 60 s. This procedure dispersed the compound in the form of both emulsion droplets and oil lenses floating on the surface of the surfactant solution (see below). Compound A was also rather active at this concentration—the foam produced during the shakings in a given cycle disappeared for about 5 s after the agitation stopped.

Methods. *Surface Tension.* The surface tension measurements were performed by the Wilhelmy plate method using a Kruss K12 tensiometer and a platinum plate. Before each measurement the plate was cleaned by heating in a flame and by immersion in hydrofluoric acid. All the experiments were carried out at an ambient temperature of 23 ± 1.0 °C.

Liquid Film Observation. Several complementary techniques were applied to observe the process of foam film rupture by antifoam particles. Some of these observations were made with a conventional video camera (Panasonic WV-CD20, 25 frames per second), while other experiments were performed with a special high-speed video camera (HSV-1000, NAC Europe, 500 or 1000 frames per second):

(a) Dippenaar Method. This method was first applied by Dippenaar[29] for observation of the foam lamella destruction caused by hydrophobic solid particles (see Figure 2). In our experiments we used this technique to observe the evolution of an oil bridge, formed when a drop of compound A bridges the two surfaces of a foam lamella. Briefly, a drop of the AOT solution was placed in a short capillary tube (in our experiments the internal diameter of the capillary was 4 mm and its height was 3 mm). The drop acquired a biconcave shape with the thinnest region being in the center of the capillary. When a drop of the antifoam compound (2 microliters in volume) was placed on the upper surface of the surfactant solution, it formed a floating lens which was held by gravity in the center of the meniscus. The amount of the surfactant solution in the capillary could be precisely controlled (thus changing the thickness of the aqueous layer) by sucking liquid in or out through the side orifice in the capillary wall (for this purpose we used a steel needle connected via plastic tube to a 1 mL syringe driven by a micrometric screw). When the thickness of the aqueous layer became equal to the penetration depth of the oil lens, an oil bridge was formed and its evolution was further monitored. The bridge was observed in transmitted light with a long-focus magnifying lens (CTL-6, Tokyo Electronic Industry Co., Ltd.; magnification ×6, working distance 39 mm) connected to a video camera. As suggested by Dippenaar,[29] the optical aberration created by the curvature of the capillary wall was eliminated by attaching a flat microscope cover glass to the capillary wall, in front of the observation system (see Figure 2). The experimental cell was closed in a small isolating box (3 × 3 × 2 cm^3) with optically clean windows to eliminate the convection of air and the evaporation of water.

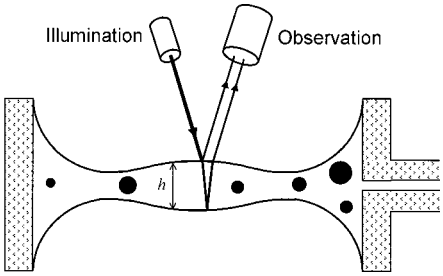

Figure 3. Origin of the interference pattern in the Scheludko cell.[33,34] Two monochromatic light beams reflected from the upper and lower film surfaces, respectively, interfere with each other. As a result, a set of bright and dark fringes corresponding to constructive or destructive interference are observed. The shape of the film surfaces can be reconstructed as explained in the text.

The main advantage of the Dippenaar cell is that it allows one to directly observe the shape of an oil bridge; however, such observations are only possible when the antifoam drop is relatively large (drop diameter on the order of 100 μm and above). The particles in the typical antifoam formulations have a diameter <10 μm, which is below the attainable resolution in these observations. Therefore, the conclusions drawn from the observations in the Dippenaar cell should be further tested with other experimental methods.

(b) Scheludko Method. This method was proposed by Scheludko and Exerova[33,34] in the late 1950s and has been widely used[35] for studying the stability and the rate of thinning of liquid films. The construction of the Scheludko cell is essentially the same as that of the Dippenaar cell. A foam film is formed from a biconcave drop placed in a short capillary (internal diameter 2.5 mm, height 4 mm in our experiments) by sucking out liquid through a side orifice. The most important conceptual difference of the Scheludko cell is that the foam film is observed in monochromatic reflected light; that is, the film is illuminated and observed in a direction perpendicular to its surfaces (Figure 3). The interference of light reflected from the upper and lower surfaces of the foam film leads to the appearance of dark and bright interference fringes, each of them corresponding to a given film thickness. The difference Δh in the film thickness between two neighboring dark (or two neighboring bright) fringes is equal to

$$\Delta h = \lambda/2n \approx 203 \text{ nm} \qquad (5)$$

where $\lambda \approx 540$ nm is the wavelength of the illuminating light and $n = 1.33$ is the refractive index of the surfactant solution. One can easily distinguish changes in the film brightness on the order of $\Delta h/4$ (bright to gray, gray to dark, and so on). Therefore, changes in the film thickness on the order of 50 nm can be easily detected

(33) Scheludko, A.; Exerova, D. *Kolloid Z.* **1957**, *155*, 39.
(34) Scheludko, A. *Adv. Colloid Interface Sci.* **1967**, *1*, 391.
(35) *Thin Liquid Films: Fundamentals and Applications*; Ivanov, I. B., Ed.; Marcel Dekker: New York, 1988.

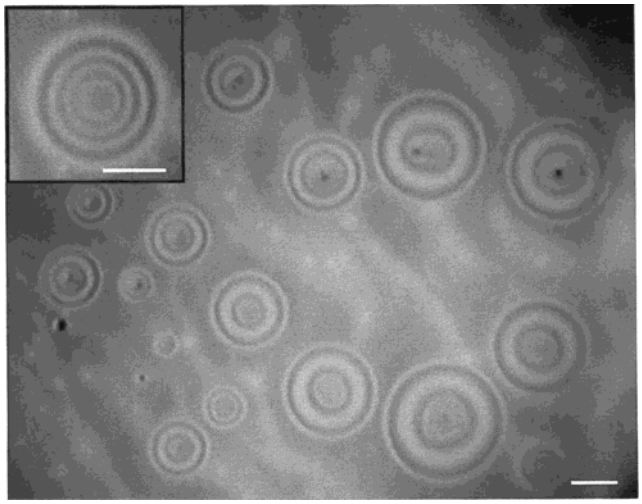

Figure 4. Lenses of compound A floating on the surface of an AOT solution as seen in reflected monochromatic light. The lenses deprived of visible silica particles (see the inset) are flatter, and the three-phase contact angle water−oil−air can be precisely calculated from the reconstructed lens shape. Most of the lenses, however, contain a lump of silica in the center which significantly increases their penetration depth. Bar = 100 μm.

in this way. More refined procedures of light intensity detection[33,34,37,38] can lead to even higher accuracy in the film thickness determination (not necessary for our tasks).

Fiber optic illumination of the film (GLI 154, FORT S. A.) and a long-focus lens (CTL-6, as described above) attached to a conventional or high-speed camera were used for these observations. As discussed elsewhere,[39] the use of an external light source for illumination (not connected to the optical system for observation of the film) has some advantage by ensuring better contrast of the interference pattern. The latter is particularly important in the experiments with a high-speed camera, where a higher intensity of the illuminating beam is required.

The major advantage of the Scheludko cell is that experiments can be performed with actual antifoam substances, dispersed into micrometer-sized droplets or lenses, just as in the case for practical antifoams. Thus, the films in the Scheludko cell closely mimic the behavior of relatively small films (diameter around 1 mm) in the real foams.

(c) Large Vertical Films Suspended on a Frame. This complementary method allows the study of relatively large foam films (up to several centimeters). A rectangular glass frame (2 cm wide, 3 cm high, produced from a glass rod of diameter 3 mm) was used, which was attached to a specially designed sliding mechanism. The latter was driven by a powerful elastic spring, which ensured reproducible rapid withdrawal of the frame from the surfactant solution (within 40−50 ms). This corresponds to a rate of about 250 cm^2/s for creating a new surface, which is comparable with the rate of fresh surface production in the Shake-Test mentioned above.

The surfactant solution and the frame were kept in a closed glass container (to reduce the evaporation of water from the films) with optically clean front and rear walls. The vertical films were observed in reflected light. White polychromatic light from a stroboscope (ST250-RE, PHYLEC) was used when the position of film rupture by the antifoam particles had to be monitored. A rectangular diaphragm (4 × 5 cm^2) was placed at the exit of the stroboscope to reduce the background illumination. Alternatively, laser monochromatic light (10 mW He−Ne laser operating at 632.8 nm; Melles Griot) was used when the dynamics of film thinning was studied. The laser beam was expanded to a diameter of about 4 cm in the plane of the foam film by means of a homemade beam-expander. In this case, the changes in the film thickness were registered by using the interference pattern, similarly to the experiments in the Scheludko cell (Δh = 238 nm in this case). A long-focus zoom lens (LMZ 45C5, ×6, 18−108 mm, F2.5; Japan Lens Inc.) attached to the high-speed camera was used in these experiments.

Microscope Observations of the Surface of the Working Solution. Observations of the surface of the surfactant solution were performed after dispersing the antifoam and before starting the thin film experiments, to check for the presence of oil lenses which could also (along with the emulsified compound) destroy the foam. The observations were performed in reflected light to enable detection of the interference pattern created by the interference of the light reflected from the upper (oil−air) and lower (oil−water) interfaces of the lens. The optical system described above for observing foam films in the Scheludko cell was used in these experiments as well. From the interference pattern we restored the shape of the floating lens and calculated the three-phase contact angles at the lens periphery. Equation 5 was used to calculate the local thickness of the oil layer in the lens (with n = 1.40 being the refractive index of the oil), and the two interfaces (oil−water and oil−air) were approximated with spherical surfaces; that is, the gravity effects were neglected.

All of the components that were in contact with the surfactant solutions were made of glass (all joints were thermally fused). Before each experimental run, the glassware was cleaned by immersion in an ethanolic solution of KOH (at least for 12 h), followed by copious rinsing with deionized water.

Table 1. Surface Tension of 10 mM AOT Solutions and Approximate Thickness of the Spread PDMS Layer in the Presence of Emulsion A[a]

system	surface tension (mN/m)	$\Delta\sigma$ (mN/m)	layer thickness (nm)
no antifoam	27.85 ± 0.05	0	0
0.01% emulsion A	25.0−25.45	2.4−2.85	>2
0.01% emulsion A loaded by TTP[b]	27.8 ± 0.05	≈0.05	<0.8
0.01% emulsion A loaded by TTP (12 h later)	24.95−25.0	≈2.9	>2

[a] The layer thickness is estimated from the measured surface tensions and the data of Bergeron and Langevin.[40] [b] TTP: two-tips procedure, which ensures a solution surface free of oil (see the text).

Results

In this section we present a summary of the main results obtained by the listed experimental methods. The analysis of these results with respect to the mechanism of antifoam action is presented in the subsequent Discussion section.

Surface Tension and Microscope Observations of the Surface of the Working Solutions. *Compound A.* Microscope observations showed that after the foaming procedure used to disperse compound A (in the Shake-Test) was completed, a part of the compound was dispersed in the form of emulsion droplets, while another part still remained on the surface of the surfactant solution in the form of floating lenses. The emulsion droplets were very polydisperse, covering the size range from 1 to 50 μm. The oil lenses were also very polydisperse in diameter, and most of them contained agglomerates of silica particles in the center—see Figure 4. The equilibrium three-phase contact angle water−oil−air was calculated from the interference fringes seen in reflected monochromatic light; a very small value, α_O = 0.4°, was found.

The surface tension of these solutions was reduced by 2.5 to 3 mN/m, compared to the tension of the AOT solution in the absence of any antifoam (see Table 1). The data from these measurements were relatively scattered (±0.5 mN/m), due to the presence of oil lenses on the solution

(36) Born, M.; Wolf, E. *Principles of Optics*; Pergamon: Oxford, 1980.
(37) Nikolov, A. D.; Wasan, D. T.; Kralchevsky, P. A.; Ivanov, I. B. *J. Colloid Interface Sci.* **1989**, *133*, 1 and 13.
(38) Bergeron, V.; Radke, C. J. *Langmuir* **1992**, *8*, 3020.
(39) Denkov, N. D.; Yoshimura, H.; Nagayama, K. *Ultramicroscopy* **1996**, *65*, 147.

surface which hydrophobized the platinum plate during the measurements, thus affecting the results. This reduction of the surface tension indicated that the oil lenses coexisted with a thin molecular layer of spread silicone oil. This conclusion is in agreement with the results of Bergeron and Langevin,[40] who measured the surface tension of AOT solutions as a function of the spread amount of PDMS on the solution surface. These authors showed[40] that the spreading of a thin layer of silicone oil (approximately 3 nm in thickness) resulted in a reduction of the surface tension of the AOT solution by about 2.6 mN/m (see Figure 5 in ref 40). Therefore, our system contained oil lenses in coexistence with a thin oil layer (pseudo-partial wetting).

Emulsion A. The microscope observations showed that the droplets of emulsion A were well dispersed in the working surfactant solution after five shakes by hand. The diameter of the droplets was between 1 and 10 μm with an average size of 1.2 μm (by number). No macroscopic oil lenses on the surface of this solution were detected. Nevertheless, the measurements showed (see Table 1) a reduction of the surface tension by 2.6 ± 0.2 mN/m, which means that in this system we also had a spread layer of silicone oil on the solution surface. From the value of the surface tension and from the data of Bergeron and Langevin,[40] we could conclude that the thickness of the spread layer was above 2 nm. The fact that we could not see this layer in reflected light means that its thickness was not larger than approximately 10 nm. As explained in the Discussion section, this spread layer (although being of nanometer thickness) is very important for the action of the antifoam.

The prespread silicone layer probably appears as a result of two processes. First, part of the silicone oil could remain on the surface of the batch emulsion without being effectively dispersed during the production of emulsion A. Second, some of the emulsion droplets could coalesce with the air−water interface during the shelf-storage of emulsion A. Whatever is the origin of the spread oil on the surface of emulsion A, part of it could be easily transferred (e.g., on the tip of the pipet used to take an aliquot of emulsion A) to the surface of the working surfactant solutions during their preparation.

To investigate in more detail the effect of the spread PDMS layer on the foam film stability, we used a relatively simple method to remove this spread layer from the solution surface. It turned out that if we inject gently the working solution containing 0.01% of emulsion A through a narrow orifice (syringe needle or pipet tip), the tension of the freshly formed surface of the solution was equal to that of the surfactant solution in the absence of antifoam (see Table 1). This means that the layer of PDMS spread on the surface of the "mother" solution was retained during this transfer procedure and it took more than 6 h until a detectable reduction of the surface tension took place again. The reduction of the surface tension is due to a slow process of surface accumulation of PDMS, most probably resulting from coalescence of some of the emulsion droplets with the solution surface. Note that the total concentration of the antifoam was virtually unchanged by the transfer procedure. Since in most of the experiments we passed the solution with a pipet through a second pipet tip which had not been in contact with the mother solution (using in fact the second tip as a funnel with a narrow exit), hereafter, for brevity, we call this procedure the "two-tip procedure" (TTP). The TTP enabled a comparison of the film stability to be made in the presence and in the absence of a prespread layer of PDMS.

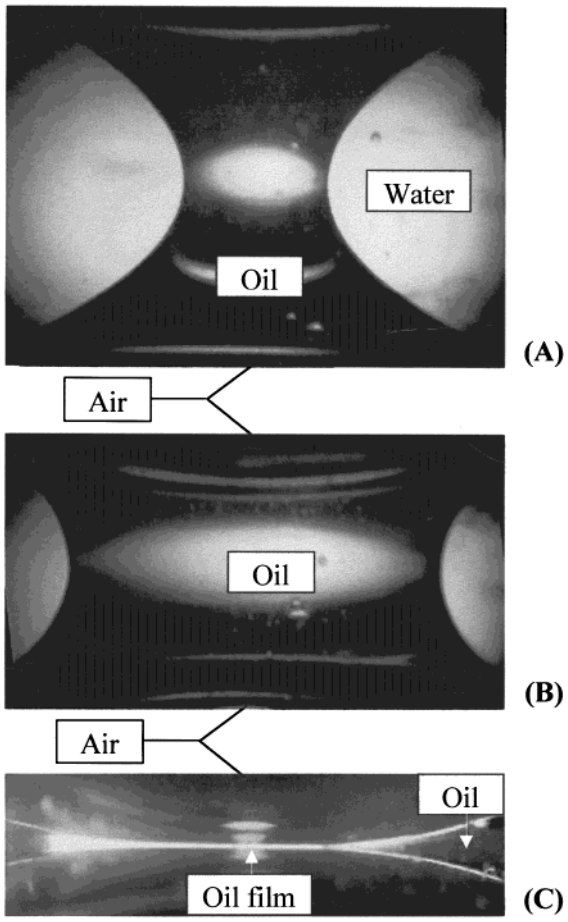

Figure 5. Bridge of compound A in the Dippenaar cell. The photographs present three consecutive stages of bridge stretching. A thin oil film is seen in part C which forms just before bridge perforation.

Bridge Shape of Compound A in the Dippenaar Cell. Dippenaar[29] used in a spectacular way the setup shown in Figure 2, to observe the process of foam lamella destruction by hydrophobic solid particles. He recorded the rapid process of bridging−dewetting with solid particles and analyzed how particle shape affects antifoam action. Our initial idea was to observe the dewetting of lenses of compound A in a similar way. However, instead of a rapid process of dewetting, we observed the formation of a relatively stable biconcave oil bridge—see Figure 5. By changing the amount of the surfactant solution in the capillary, we were able to reversibly stretch (in a radial direction) or contract the bridge, which means that the bridge was in mechanical equilibrium (the capillary pressures across the interfaces were balanced and the contact angles at the three-phase contact lines were satisfied). Only after excessive stretching of the bridge did a thin oil film form in its center, which resulted in rapid rupture of the bridge.

The most important conclusion from this observation is that the dewetting is not the only possible scenario for foam film destruction by oil lenses. In fact, the deformability of the oil phase results in the formation of a biconcave bridge, like that shown in Figure 5, which cannot be dewetted. The conditions for stability of deformable oil bridges in foam films are discussed in detail in the second part[18] of the study.

On the other hand, as mentioned above, the antifoam lenses observed in the Dippenaar cell are much larger

(40) Bergeron, V.; Langevin, D. *Macromolecules* **1996**, *29*, 306.

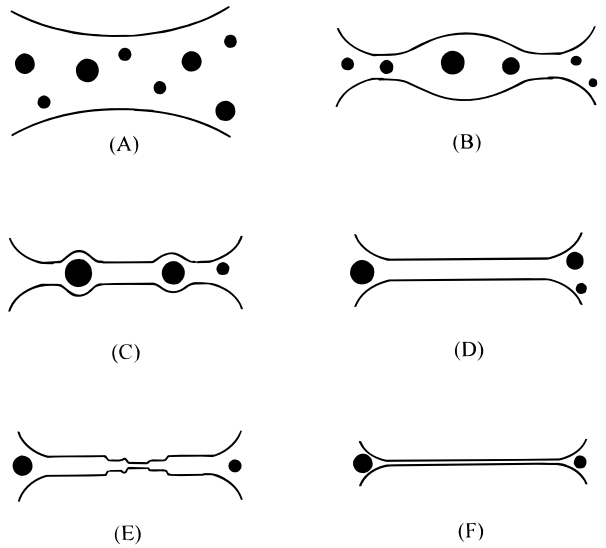

Figure 6. Schematic presentation of the main stages of foam film evolution as observed in the Scheludko cell. Two concave surfaces approach each other (A) and first form a film with a thicker central region surrounded by a thinner boundary (B). This lens-shaped configuration is called a "dimple",[35] and it is hydrodynamically unstable. After the expulsion of the dimple, an almost planar film crossed by several thicker regions (channels) is formed (C). With the further film thinning, the channels disappear (D). Several stepwise transitions are observed in a process called "stratification"[37,38] at film thickness < 100 nm (E). The film eventually reaches its equilibrium thickness (F). If the film is not destroyed by antifoam particles during stages A−C, the particles leave the film (due to their relatively large size) and it remains relatively stable.

than the antifoam particles found in the working solutions. The dynamics of film thinning and the respective time scales are also very different. For these reasons, the observations in the Dippenaar cell only suggest another possibility for film destruction but cannot be used as decisive proof for the mechanism of foam destruction. Experiments with well-dispersed compound A and emulsion A in the other experimental cells were needed to define unambiguously which of the possible mechanisms is realized in practice.

Stability of Small Foam Films in the Scheludko Cell. In these experiments we observed the process of foam film destruction by emulsified antifoam particles (emulsion A and compound A) or by antifoam lenses floating on the film surface (compound A). The antifoams were dispersed in the working surfactant solutions as described in the Experimental Section.

For reference, we first describe briefly the main stages of foam film thinning in the absence of antifoam. Films of diameter between 0.6 and 0.8 mm were studied. Just after their formation, the films had a nonuniform thickness with a thicker lens-shaped region (usually called a dimple) in the center—see Figure 6. From the interference pattern we could determine the film thickness in the center of the dimple to be about 3−4 μm, while the thinner region in the film periphery was 1−1.2 μm thick. The dimples were hydrodynamically unstable and spontaneously left the film a few seconds after it was formed. The film was about 0.8−1 μm thick after dimple expulsion and contained several channels (dynamic regions with thickness 200−500 nm larger than the surrounding planar portions of the film). The film gradually thinned down to 100 nm in about 45 s, and the channels almost disappeared at that thickness. Further, we observed two consecutive sharp stepwise transitions in the film thickness through a formation and expansion of thinner spots. Such a method of liquid film thinning is called "stratification" in the literature[37,38,41−44] and comes about due to oscillatory structural forces, created by the micelles. Apparently, 2.5 min after its formation, the film reached its final state, a common black film (thickness of about 10−20 nm), and was extremely stable in the absence of antifoams.

Emulsion A. The overall thinning pattern of the foam film was not substantially affected by the presence of antifoam particles—the same main stages were observed within approximately the same time scale. However, in many cases the antifoam particles caused rupture of the foam film at a relatively large thickness. Since the film stability depended very much on the presence of a prespread layer of PDMS on the film surfaces, we describe first the general phenomena and then specify the differences in the experiments with and without a spread layer.

Typically between 5 and 10 antifoam particles (seen as dark dots in reflected light) were captured in the dimple immediately after foam film formation. Most of these particles left the film together with the dimple. However, several new particles were seen to enter the foam film from the surrounding meniscus region. These particles were dragged into the film by liquid circulation, which accompanied the dimple expulsion. With further film thinning, the particles moved from the planar film areas toward the channels (where the film thickness was larger) and then left the film, following the drainage of liquid through the channels. Often other antifoam particles were "sucked in" the film by liquid circulating around the channels' contacts with the surrounding meniscus. At smaller film thickness (100 nm and below), practically all visible antifoam particles were already expelled from the film into the neighboring thicker meniscus region (Figure 6).

Note that in these observations the antifoam droplets served as tracers for visualizing the liquid flow in the film. The observed dynamics of liquid drainage at large film thickness was much more complex than the simple picture of a gradually thinning plane-parallel film—an intensive circulation of liquid in the plane of the film (especially at the boundary with the surrounding meniscus region) was observed. This resulted in an intensive exchange of particles between the film and the meniscus, which facilitated the particle entry and the subsequent bridge formation and film rupture.

(a) Foam Films in the Presence of a Prespread Layer of Oil. For these experiments the Scheludko cell was loaded by using one tip on the pipet. As indicated from the surface tension measurements, such a transfer of the solution is accompanied by some transport of spread oil from the "mother" solution into the Scheludko cell.

In general, the foam films in these experiments were rather unstable—practically all of them were destroyed within 1−10 s by the antifoam particles, at a relatively large film thickness and at different stages of the film evolution (mostly in stages B and C in Figure 6). One important feature of the observed processes was the formation of a characteristic interference pattern just before the film rupture—see Figure 7. For brevity, this characteristic visual appearance will be termed a "fish-eye". This pattern indicated local reduction of the foam

(41) Pollard, M. L.; Radke, C. J. *J. Chem. Phys.* **1994**, *101*, 6979.
(42) Chu, X. L.; Nikolov, A. D.; Wasan, D. T. *Langmuir* **1994**, *10*, 4403.
(43) Kralchevsky, P. A.; Denkov, N. D. *Chem. Phys. Lett.* **1995**, *240*, 385; *Prog. Colloid Polym. Sci.* **1995**, *98*, 18.
(44) Kralchevsky, P. A.; Danov, K. D.; Denkov, N. D. In *Handbook of Surface and Colloid Chemistry*; Birdi, K. S., Ed.; CRC Press: New York, 1997; Chapter 11.

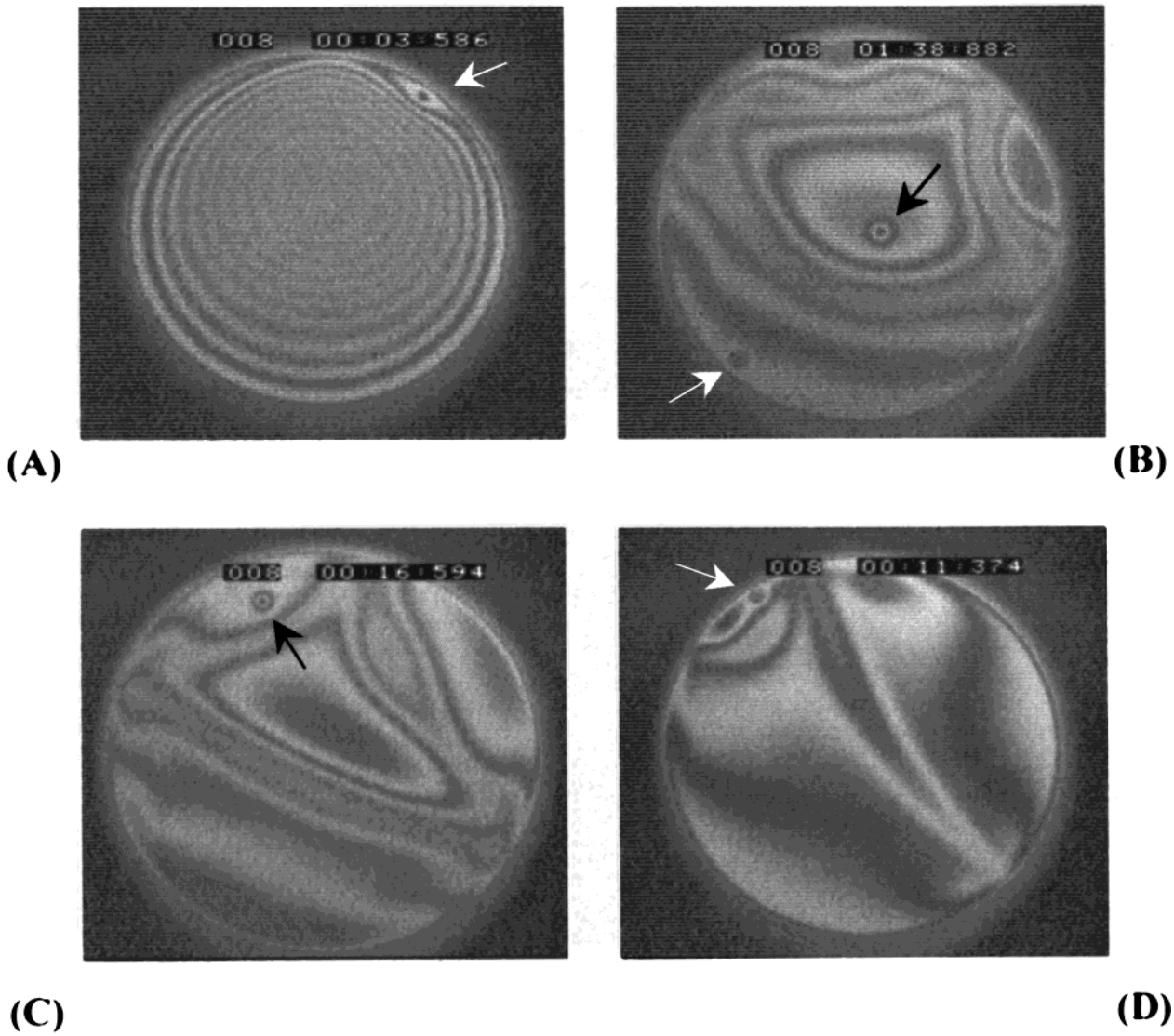

Figure 7. Interference pattern (see the arrows) indicating the formation of oil bridges in foam films just before their rupture (Scheludko cell). The film in part A contains a dimple (stage B in Figure 6), while the films in parts B to D contain channels (stage C in Figure 6). The films are made from an AOT solution containing 0.01% emulsion A.

film thickness by 100−300 nm. The perturbed film region was localized (10−50 μm in diameter), and the rest of the film thinned without being notably affected by its presence. The position of bridge formation was usually close to the dimple periphery—in the thinnest region surrounding the dimple (stage B in Figure 6) or at the boundary of the film-containing channels (stage C). This tendency was further enhanced by the liquid circulation, which forced particles to enter into the film from the thicker meniscus region. Statistically less probable (but still often observed) was the bridge formation in the planar portions of the film. Typically, the film ruptured soon after the appearance of the first fish-eye. Occasionally, one could see the formation of two or even three fish-eyes in one and the same film before it ruptured. In most cases one could unambiguously point out the antifoam particle which transformed into a bridge.

We could distinguish two types of fish-eyes: (i) inherently unstable, which rapidly and continuously expanded in diameter, leading to an almost instantaneous film rupture (within several milliseconds after the bridge was formed), and (ii) metastable, which changed slowly their shape over a longer period (from fraction of a second up to several seconds) but afterward suddenly and rapidly expanded and ruptured the film. As discussed in the second part of this study,[18] these two cases correspond to mechanically unstable and metastable bridges, respectively. The theoretical analysis showed that the oil bridges could be mechanically stable even at positive values of the bridging coefficient B if the film thickness at the moment of bridge formation is comparable with the diameter of the oil droplet (or larger). Another factor that could lead to bridge stabilization is the presence of silica particles, but this effect is very difficult to quantify. Therefore, case (ii) corresponds to a transition from a metastable bridge to a mechanically unstable bridge due to the reduction of the foam film thickness or to some other processes which are discussed in ref 18.

The characteristic interference patterns described above (the fish-eyes) could not be caused by spreading of PDMS from the antifoam droplets, because the foam−film surfaces were already saturated with oil. Moreover, we noticed that larger amounts of oil on the film surfaces lead to faster bridge evolution and film rupture (viz. the results for compound A described below)—if the interference pattern was caused by oil spreading from the antifoam droplet, one should expect the reverse trend. Furthermore, if the fish-eyes were due to oil spreading, one could expect

that they would change continuously with time and would disappear as soon as the oil was completely spread over the film surface (if the foam film is still intact). As discussed in the second part of the study,[18] the oil bridges in foam films can be metastable for a certain period of time, just as observed in the experiment. Therefore, we can conclude that the fish-eyes indicated the formation of oil bridges, probably containing some silica as well.

Note that the fish-eyes are much larger (diameter 10−50 μm) than the actual oil bridges, whose size, typically several micrometers, should be comparable to or slightly larger than the film thickness. The fish-eyes are larger because they include not only the oil bridge but also the deformed film surfaces surrounding the bridge. Examples of calculated shapes of the bridge and the contiguous film surfaces are given in the second part of the study.[18]

(b) Foam Films in the Absence of a Prespread Layer of PDMS. In these experiments the Scheludko cell was loaded by using the two-tip procedure (TTP), which ensured film surfaces free of a spread oil layer. Remarkably, this "small" change in the loading procedure had a tremendous effect on the film stability—in most of the experiments, the antifoam particles left the foam film without making bridges and without rupturing it. As a result, the films were rather stable.

In some cases we observed the characteristic interference pattern indicating the formation of a bridge, but typically these bridges were stable. They moved to the periphery of the foam film, and a transient local decrease in the film thickness (about 100−150 nm less than the remaining area of the film) was observed around the bridge. This decrease in the film thickness most probably indicated a process of oil spreading from the bridge (note that the film surfaces were not saturated with oil in these experiments). Within several seconds the film restored its local thickness and afterward only the "remains" of the bridge (probably silica particles with some residual oil) could be seen at the film periphery as a small dark dot without notable effect on the further film-thinning process. Very rarely the bridge formation lead to a film rupture under these conditions.

In several cases we observed entry of a droplet into one of the film surfaces (without bridge formation) and subsequent spreading of the oil around the entry spot. The spreading of the oil was visualized by rapid change (within several milliseconds) of the interference pattern corresponding to local thinning of the foam film. However, the local interference pattern disappeared after a short period of time (within a second). We did not register any rupture of foam films as a result of the spreading process.

Compound A. The thinning pattern and the stability of foam films in the presence of compound A were similar to those reported above for emulsion A. The surfaces of the films obtained after loading the Scheludko cell with the TTP were free from floating lenses and from a spread oil layer. These films were relatively stable, although many drops of emulsified compound A were seen in the solution. During the process of film formation one could trap some of these emulsion droplets, but they left the film without rupturing it. In general, the probability of trapping drops of compound A in the foam film (1−2 particles) was substantially smaller than that for emulsion A, because the particle number concentration was lower. Another reason for this reduced probability could be the larger size of the drops from compound A, that were expelled from the film region before the film was formed.

The surfaces of the films obtained after loading the Scheludko cell with one tip on the pipet were covered with many small oil lenses (diameter up to 100 μm), which were obviously transferred by the pipet tip from the surface of the "mother" solution. The interference pattern from these films was quite complex, because it presented a superposition of three different interferences: one due to the water−air interfaces (film surfaces) and two others created from the oil lenses floating on both film surfaces. Nevertheless, after some practice one could "decompose" the interference pattern and analyze the processes leading to its change (dimple formation and expulsion, bridging, and so on). These films were very unstable and ruptured for <1 s at a thickness > 1 μm. In most cases it was possible to identify the position of bridge formation and film rupture—not surprisingly, it was observed that both the emulsified drops and the oil lenses could transform into oil bridges and rupture the film. A typical time sequence of the film rupture process by an oil lens is shown in Figure 8. Remarkably, in all cases the film ruptured very rapidly (within 2−10 ms) after the bridge was formed; that is, these bridges were mechanically unstable in the notation discussed above. In these experiments, long-living (metastable) bridges, as found with emulsion A, were not observed.

Let us summarize here several observations, which are not consistent with the bridging−dewetting mechanism of film rupture. The first observation comes from the details of the rupture process as seen with the high-speed camera. As shown in Figure 8, very often we observed the formation and expansion of a dark spot in the center of the bridge. These spots rapidly expanded up to a diameter of 10−40 μm (within several milliseconds), and immediately after that the foam film ruptured. Similar dark spots were often observed in the bridges formed from the droplets in emulsion A (i.e., these dark spots are a characteristic of bridges formed from either lenses or emulsion droplets). The only explanation we could envisage for these spots is that they correspond to very thin microscopic oil films (analogous to that shown in Figure 5C), which in fact is the final stage of bridge stretching before it ruptures. Indeed, their dark appearance shows that their thickness is <50 nm. We rule out the possibility that these spots are just holes in the film, because the rate of hole expansion would then be extremely high (several mm/ms—see eq 6 below) and this process could not be followed experimentally. Therefore, we can conclude that the evolution of bridges formed in the Scheludko cell follows the evolution observed in the Dippenaar cell (but at completely different time and size scales).

Another argument against the bridging−dewetting mechanism for our system is that the dewetting process is too fast to be observed with our equipment. The experiments of Dippenaar[29] with solid particles showed that the speed of the three-phase contact line along the particle surface was on the order of several micrometers per second (e.g., a glass bead of radius 80 μm was dewetted for 10 ms). This speed could also be theoretically estimated on the basis of some existing theories,[45,46] and these estimates predict values well above 1 μm/ms. This means that the dewetting process in the case of our small particles should last for <1 ms, and with the present experimental setup, the interference pattern accompanying it could not be seen.

Large Vertical Films Suspended on a Frame. In these experiments we studied the stability of vertical, relatively large films (2 × 3 cm^2). In general, these films were much more unstable at the same antifoam concen-

(45) Ivanov, I. B.; Dimitrov, D. S. Chapter 7 in ref 35.
(46) Ivanov, I. B.; Dimitrov, D. S.; Radoev, B. P. *J. Colloid Interface Sci.* **1978**, *63*, 166.

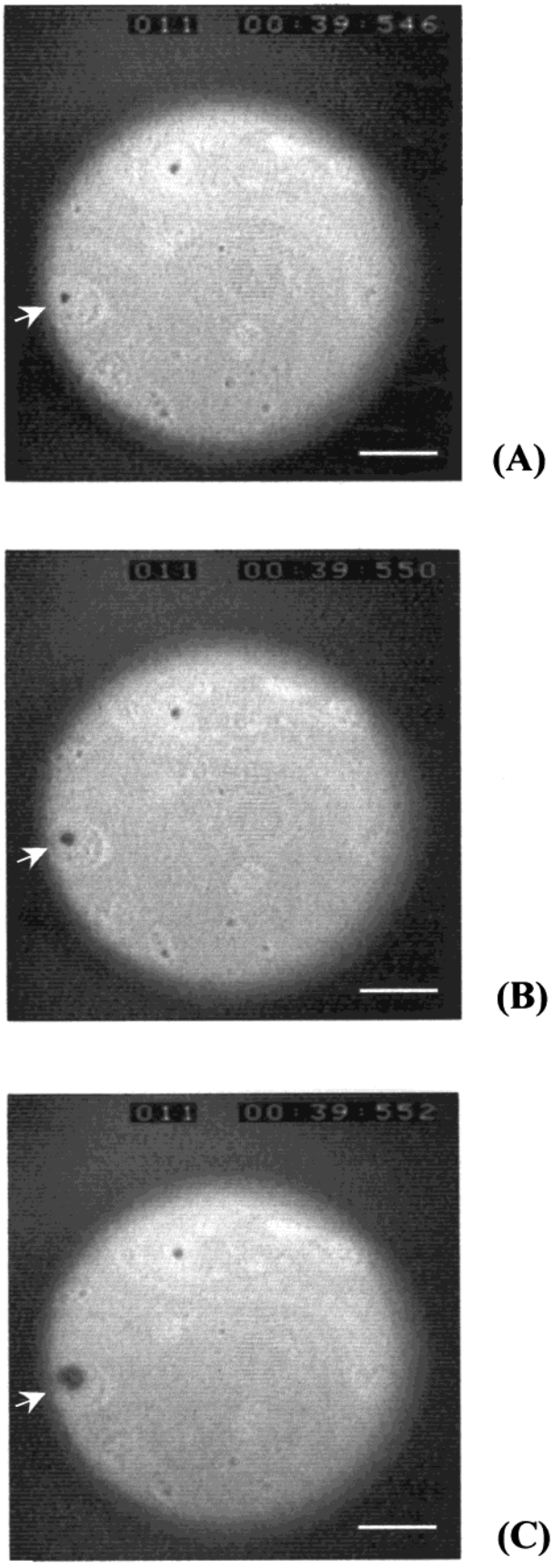

Figure 8. Bridge formation and stretching in the presence of compound A. The bridge is formed from an oil lens containing a lump of silica (the dark dot indicated by an arrow in part A). The rapid stretching of the bridge (see the increase of the dark spot, which presents a very thin oil layer, cf. Figure 5C) leads to film rupture within 4 ms. Bar = 100 μm.

tration (0.01 vol %), because the probability to trap antifoam particles was much higher. If we assume that the probability for capturing particles in the moment of film formation is roughly proportional to the film area, we can estimate that at least 5000 particles (some of them being substantially larger than the average size) were captured in the large films. Not surprisingly, these films ruptured almost immediately (within 0.1−0.5 s) after their formation. To analyze in more detail the process of film destruction, we performed also experiments at reduced antifoam concentration (0.0012 vol %) and in the absence of antifoam. For technical reasons it turned out to be impossible to perform experiments in the absence of a prespread layer of PDMS. With compound A it was impossible to produce a large volume of the working solution needed to load the container for these experiments (400 cm^3) with the surface clean of PDMS. Surface tension measurements showed that, after passing approximately 50 mL of the solution containing 0.01% compound A by means of the TTP, the surface of the solution was already covered with a thin layer of oil (note that about 0.1 mL of solution is needed for the Scheludko cell, so that this problem was not important there). Most probably, this oil appeared from the coalescence of some of the antifoam droplets with the solution surface. With emulsion A it was possible to produce a clean surface and to start the experiment, but after formation and rupture of several films, the surface tension of the solution decreased, which indicated the presence of PDMS on the solution surface. Therefore, all the experiments discussed below (except those in the absence of any antifoam) correspond to the case when a spread oil layer already existed on the solution surface.

Dynamics of Vertical Film Thinning in the Absence of Antifoam. Since the vertical films ruptured very soon after their formation (in the presence of antifoams), we were particularly interested in the early stages of film thinning. The combination of a high-speed camera and laser illumination gave us the unique possibility to observe the interference pattern immediately after the films were formed and to monitor in great detail the initial stages of film thinning (Figure 9).

The fast withdrawal of the frame from the surfactant solution (for about 50 ms) was often accompanied by a splash of liquid which fell down for another 100 ms. Afterward a relatively homogeneous central zone in the film was formed with thinner portions at the film periphery (Figure 9A). One can speculate that this stage corresponded to the process of dimple formation in the case of small horizontal films. This huge dimple was hydrodynamically unstable, and after several tenths of a second we observed the appearance of turbulent eddies in the lower part of the film, which gradually (for about 0.4 s) expanded and occupied the whole film area (Figure 9C). For a period of about 0.8 s the film was very inhomogeneous (turbulent) in thickness (Figure 9D). Then a gradual smoothening of the film was observed with the formation of the characteristic gradient in the film thickness due to gravity (Figure 9E) (about 3 s after the film formation). At the end of this stage we observed a second generation of turbulent eddies in the lower part of the film which further expanded and covered the peripheral zones of the film (Figure 9F); in fact, this was the generation of the so-called "marginal regeneration zone" (another 2 s). Thus 4−5 s after the film was formed, we had a very homogeneous central region (with a gradual decrease of the film thickness in the vertical direction) surrounded by the turbulent marginal regeneration zones. The film continued to thin down, and about 30−40 s later, a thin

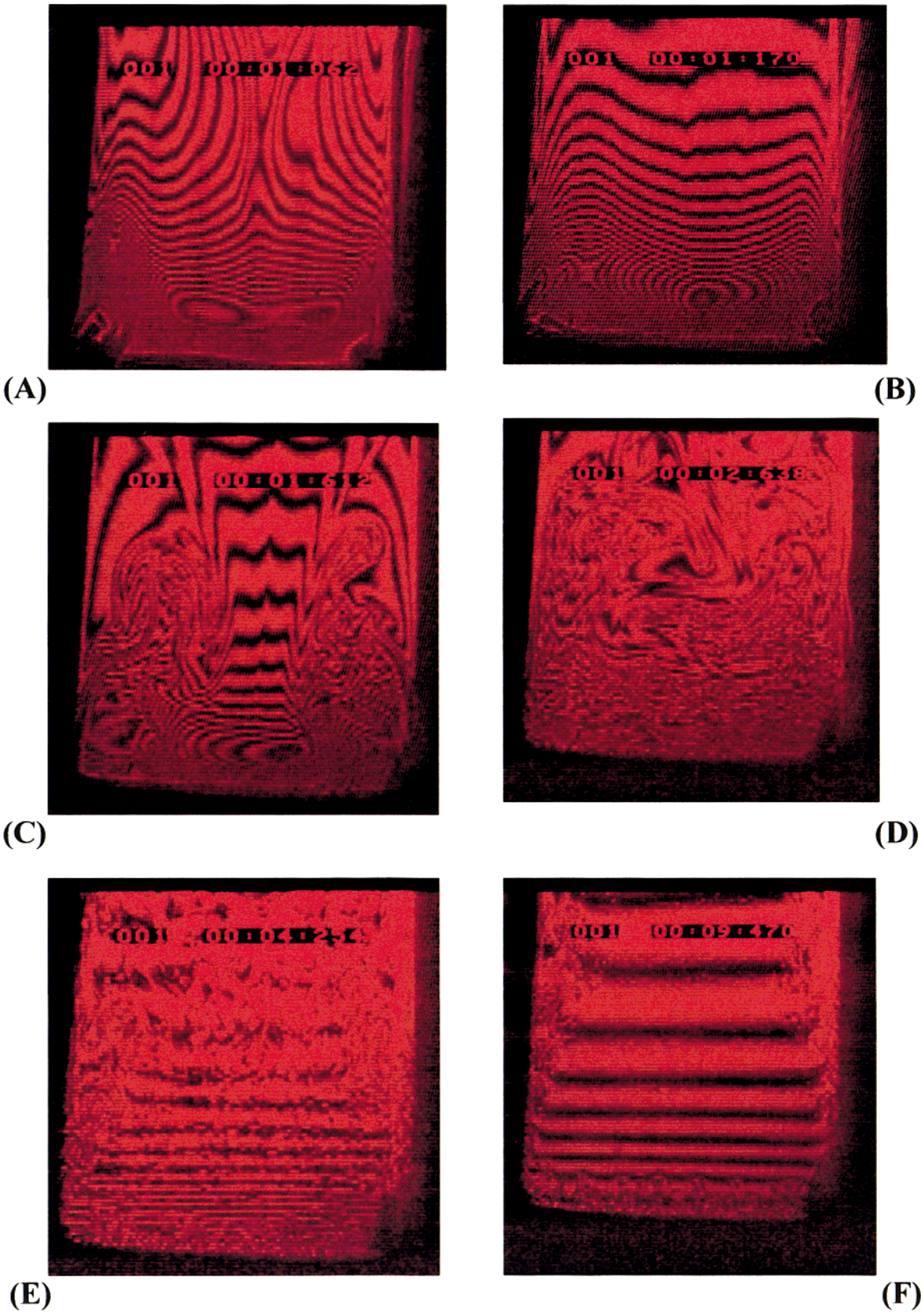

Figure 9. Different stages of thinning of a centimeter-sized vertical foam film (in the absence of any antifoam). The interference stripes indicate regions of equal thickness similarly to the curves on a topographic map. Initially, a relatively homogeneous in thickness zone is formed in the center of the film, surrounded by thinner portions at the film periphery (A). The gravity leads to gradual thinning of the upper portion of the film (B). Turbulent eddies appear in the lower part of the film (C), which develop and occupy the film area, thus making the film thickness nonuniform (D). Afterward, the inhomogeneities slowly disappear (E) and the typical gradual decrease of the film thickness with height is established due to gravity (F). Later, a thin black region appears in the upper part of the film (not shown), and finally the film ruptures.

black region was seen to appear in the upper part of the film. The film ruptured about 1−2 min after the appearance of the dark spots. We cannot exclude the possibility that the film rupture was facilitated by some (although not very intensive) evaporation of water from the film. The container in which the vertical films were formed was relatively large in volume (to ensure good conditions for optical observations), and it was extremely difficult to eliminate completely the evaporation and to obtain very long-living large films. However, the effect of water evaporation on the initial stages of film thinning (when the film was still thick) was certainly negligible.

Stability of Vertical Films in the Presence of 0.01 vol % Antifoam (Position of Film Rupture). These experiments were performed with emulsion A, and 19 films were observed. To detect precisely the position of film rupture, illumination in reflected polychromatic (white) light was used—see Figure 10. In all of the cases, the films ruptured within 0.5 s after their formation at a thickness of several micrometers. The film lifetime in most of the cases was between 0.1 and 0.3 s. To make a more precise classification of the position of film rupture, the film was subdivided into two regions of equal area—a boundary region along the periphery of the film (band having a width of 3.5 mm) and a central region (of dimensions 13×23 mm^2). It was found that the film rupture started in the central region in 35% of the experiments (7 films), while the rupture was in the boundary region (but still in the film area) in 65% of the experiments (12 films). Such a tendency could have been anticipated, having in mind the smaller film thickness in the boundary region at the early stages of film formation (Figure 9A,B). As mentioned above, a similar tendency of bridge formation and film rupture in the thinner boundary regions was observed with smaller films in the Scheludko cell as well.

Stability of Films in the Presence of 0.0012 vol % Antifoam. The aim of these experiments was to see how the process of film rupture is affected by the antifoam concentration. Such 10-fold lowering of the concentration is not unrealistic from the viewpoint of antifoam application in industrial systems. In this way we mimic also (in some aspects) the process of antifoam deactivation (exhaustion) when only part of the antifoam particles have the appropriate size and composition to rupture the films. Experiments with both emulsion A and compound A were performed. For these experiments, compound A was first dispersed as described in the Experimental Section, and then the obtained 0.01% emulsion was diluted with 10 mM AOT solution to the desired final concentration of antifoam.

(a) Emulsion A. In two independent series of experiments, 46 films were observed. About 35% of these films ruptured in the first 0.5 s after film formation. The lifetime of the remaining films was very scattered and >35% of the films lived longer than 9 s (some of the films survived up to 20 s).

The films that ruptured in the first 0.5 s also demonstrated a higher tendency for rupture in the boundary region than in the central one (ratio approximately 2:1). However, for about 30% of the short-living films it was impossible to localize exactly the position of film rupture because the hole in the film appeared exactly at the film boundary (Figure 10C). In these cases the actual rupture could be in the film (very close to the Gibbs−Plateau border) or in the Gibbs−Plateau border (GPB). With our time resolution and objective magnification it was not possible to distinguish these two possibilities. Furthermore, we could not rule out the possibility that in some of these cases the rupture took place at the glass frame (which would be obviously an artifact of the experimental

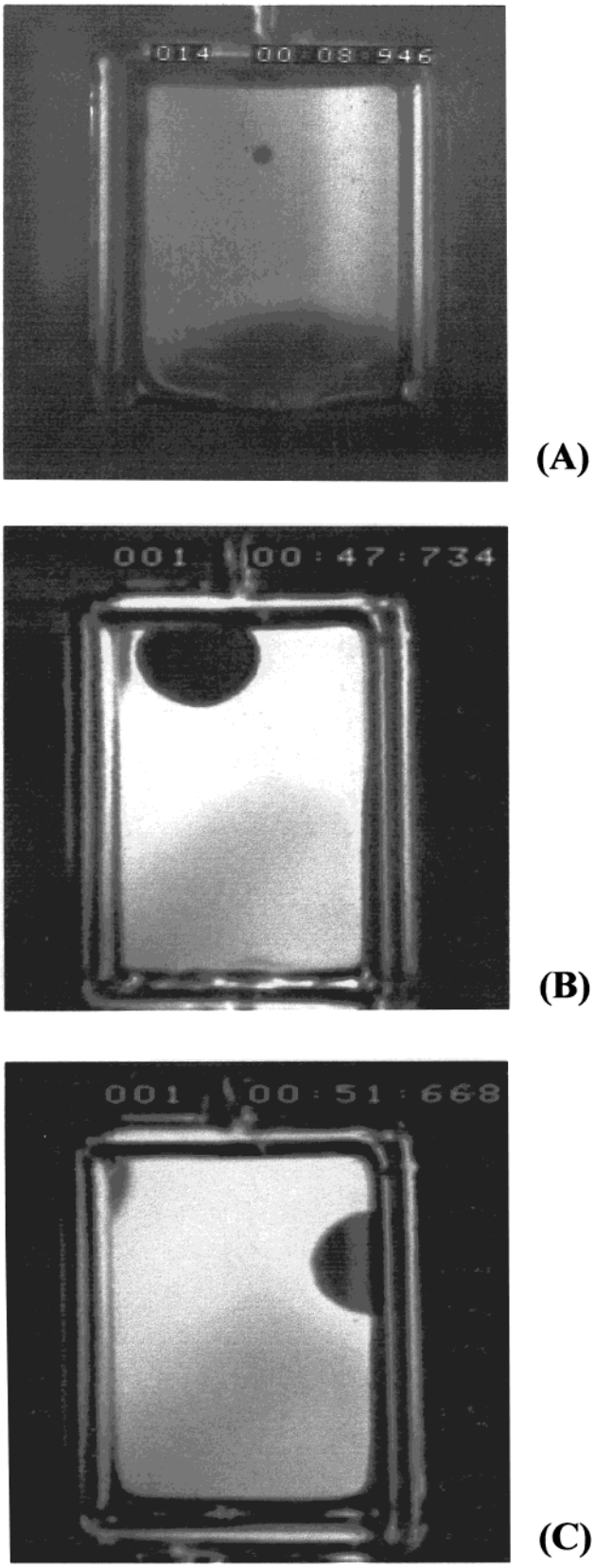

Figure 10. Rupture of vertical foam films in the presence of 0.01% emulsion A. The black spots in the film area indicate rapidly expanding holes. The hole appeared in the central region in part A and in the boundary region in part B; see the text. The exact position of film rupture cannot be distinguished in part C because the hole appeared exactly at the film boundary.

method). Nevertheless, in the prevailing number of runs (70%), the hole appeared definitely in the film area.

It was practically impossible to identify the position of perforation for the long-living films. The main reason was that these films ruptured at smaller thickness, so that the rate of expansion of the hole in the films was very high. The rate of hole expansion in a foam film is accurately described by the equation of Dupre−Culick[47,48]

$$V_H = \sqrt{2\sigma/\rho h} \qquad (6)$$

where V_H is the radial velocity of hole expansion, σ is the surface tension of the surfactant solution, ρ is the mass density of the liquid, and h is the film thickness. This equation describes rather accurately the experimental data, except in the case of extremely thin Newton-black films.[49] For our system one can estimate that V_H is 3.3 m/s for $h = 5\ \mu$m and 10 m/s for $h = 0.5\ \mu$m. With our time resolution of 1 ms we could identify precisely the position of hole appearance at V_H below approximately 5 m/s, which corresponds to film thickness $h > 2\ \mu$m.

(b) Compound A. In two independent runs, 72 films were observed. Generally, the films in the presence of compound A were more unstable than those containing emulsion A. About 55% of the films ruptured within the first 0.5 s, at relatively large thickness, and >95% ruptured within the first 3 s. Most probably, the reason for the higher activity of compound A (at the same total concentration) is the accumulation of antifoam at the solution surface. The tendency for film perforation in the *boundary* region was pronounced (boundary to central region ≈4:1). For about 35% of all films (especially for those living longer than 1 s), it was impossible to define exactly the position of film rupture—it was either in the GPB (or in the film very close to the GPB) or on the glass frame.

Discussion—Mechanisms of Antifoam Action

Comparison of Compound A and Emulsion A. There could be several reasons for differences in the antifoam action of compound A and emulsion A. One reason could be the difference in the distribution of the antifoam in the working solutions—the antifoam is entirely dispersed in the form of small droplets in the case of emulsion A (except the thin molecular layer on the solution surface), while a relatively large portion of compound A remains in the form of lenses floating on the solution surface. Another reason could be the emulsification process, used to fabricate emulsion A. The mechanical agitation during the emulsification process could lead to the formation of a particular configuration of the silica−silicone oil entities (e.g., formation of a layer of silica on the surface of the oil droplets,[12] like in the Pickering emulsions), which is absent in compound A. The typical size of the antifoam droplets is also different in these two systems. As a result, the entry of the emulsion droplets, the bridge formation, and the stability could be, in principle, different. The third reason for the different activities could be the presence of nonionic surfactants used to stabilize the concentrated batch of emulsion A (these are absent in compound A). Remarkably, all results showed basically the same mechanism of foam film rupture (bridging−stretching) with these two antifoams. The only important qualitative difference was the possibility for film bridging by a lens floating on the film surface in the case of compound A; the latter option was obviously missing in the case of emulsion A.

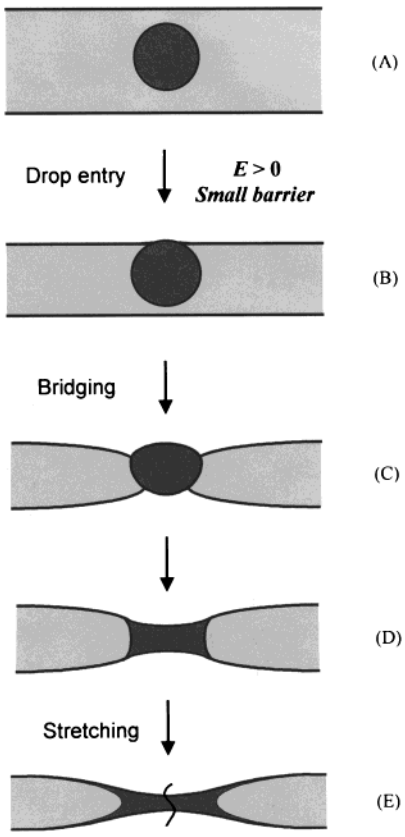

Figure 11. "Bridging−stretching" mechanism of foam film destruction. After an oil bridge is formed (A → C), it stretches due to uncompensated capillary pressures at the oil−water and oil−air interfaces (C → E). Finally, the oil bridge ruptures in its thinnest central region (the vertical wavy line in E). The driving force of bridge stretching and the respective theoretical analysis are discussed elsewhere.[18]

The most substantial quantitative difference was the higher activity of compound A (compared to emulsion A) at the same total antifoam concentration. This higher activity was detected in the model experiments with single foam films (faster rupture at larger film thickness) and in the foam stability tests performed by the Shake-Test. The faster film rupture by compound A could be easily explained with the higher concentration of the antifoam material on the film surfaces (in the form of lenses), which leads to an increased probability for bridge formation and film rupture. On the contrary, practically all of the antifoam is emulsified in emulsion A and only those particles that enter in the foam film may lead to its rupture. Our observations showed that the number of trapped particles is relatively small for millimeter-sized foam films (5−10 particles in our experiments in the Scheludko cell) and many of them leave the film without rupturing it.

The similarity of the film rupture process for emulsion A and compound A allows us to discuss their antifoam action on a common basis.

Mechanism of Film Rupture. The central question of the present study is, What is the mechanism by which the antifoam particles destroy the foam film? The results unambiguously show that we observed a process of bridge formation (either from a lens of compound A or from an emulsion drop) and further stretching of the bridge until the latter ruptures—see Figure 11. The driving force for bridge stretching is the imbalance of the capillary pressure

(47) Dupre, A. *Ann. Chim. Phys.* **1867**, *11*, 3018.
(48) Culick, F. E. C. *J. Appl. Phys.* **1960**, *31*, 1128.
(49) Evers, L. J.; Shulepov, S. Yu.; Frens, G. *Faraday Discuss.* **1996**, *104*, 335.

jumps across the three interfaces (oil−water, oil−air, and water−air).

As suggested by Garrett,[17] the stability of the bridges is primarily determined by the three-phase contact angle oil−water−air (expressed in his formalism by the value of the bridging coefficient B). As it is shown in the second part of this study,[18] the size of the oil bridge (scaled by the film thickness) is another important parameter that should also be taken into account when considering the bridge stability. Small-volume oil bridges could be stable (more precisely metastable) in the foam film even when the value of B is strongly positive. This explains why in many experiments metastable, long-living bridges (from a fraction of a second up to several seconds) were observed, which afterward suddenly expanded and within several milliseconds ruptured the film. This process corresponds to transition from a metastable bridge to an unstable bridge caused (i) by an actual increase of the bridge volume (through accumulation of oil from the spread oil layer—analogue of the Ostwald ripening in emulsions) or (ii) by a decrease of the thickness of the foam film surrounding the bridge. In addition, one could expect that the stability of the oil bridges is strongly influenced by the presence of silica particles, but this effect is very difficult to analyze theoretically.

Importance of the Values of *E*, *S*, and *B*. As discussed in the Introduction, the values of E, S, and B are often used to quantify the properties of a given antifoam oil. The fact that we are able to identify the mechanism in our particular system allows us to discuss in more concrete terms what is the importance of these coefficients for this system.

From the equilibrium values of the interfacial tensions ($\sigma_{OA} = 20.6$ mN/m, $\sigma_{OW} = 4.7$ mN/m, $\sigma_{WA} = 25.7$ mN/m) one can calculate $E = 9.6$ mN/m, $S = -0.2$ mN/m, and $B = 248$ (mN/m)^2; that is, E and B are positive, while the value of S is practically zero (in the framework of the experimental accuracy). The fact that we observe lenses on the surface of the working solutions means that the actual value of S is slightly negative. The initial values of these three coefficients (calculated from the surface tension of the AOT solution before equilibrating the surface with oil—$\sigma_{WA} = 28.5$ mN/m) are all positive: $E^I = 12.1$ mN/m, $S^I = 2.5$ mN/m, and $B^I = 376$ (mN/m)^2.

From the viewpoint of the bridging−stretching mechanism, a positive value of E is a necessary condition for formation of a bridge. Negative values of E would lead to wetting of the oil by the aqueous phase (even if the drop has appeared on the solution surface by chance) and to entire immersion of the drop back into the aqueous phase. Therefore, an antifoam would be rather inactive in the bridging−stretching mechanism if E is negative. Our observations also confirm the conclusions by Garrett[2,12] and Bergeron et al.[10] that the solid particles substantially facilitate the particle entry by reducing the entry barrier (the oil alone had very low antifoam activity in the studied solution). In addition, the silica particles substantially increase the penetration depth of oil lenses (as evidenced by the photographs shown in Figure 4), which also favors the formation of unstable bridges.

In accordance with Garrett's model[17] and our further development[18] of his approach, the formed bridges could be unstable if the value of B is positive. If B is negative, the formed bridges are stable and will not rupture the film. Note that positive values of B necessarily mean positive E (the reverse statement is not true).[10] Therefore, the requirement for positive B is a stronger condition—it includes the requirement for positive E.

The role of the spread oil layer and the values of S and S^I on the antifoam action deserves more detailed discussion. As mentioned in the Introduction, the fact that the oil spreading on the solution surface correlates to some extent with the efficiency of the antifoam has been known for many years. However, this effect is usually explained with the spreading-fluid entrainment mechanism, and positive spreading coefficients are often proposed as a necessary condition for having high antifoam activity. Our results definitely show that very active antifoam could operate without fluid entrainment and at a negative value of the equilibrium spreading coefficient S.

Furthermore, the results demonstrate the important role of the prespread oil layer for film stability. In the absence of a prespread layer, most of the antifoam particles left the films without entering, and when bridges were formed, the latter were relatively stable. On the contrary, in the presence of a prespread oil layer, the entry was easy and the foam films were unstable. Therefore, we can conclude that having a positive initial spreading coefficient S^I (which ensures a driving force for formation of a spread molecular layer) could be rather helpful for the antifoam action. From this viewpoint, the rate of oil spreading on the solution surface is another important factor for the antifoam efficiency,[10,50] because the creation of a new surface in real foams could be faster than spreading. A high spreading rate will ensure the presence of a prespread molecular layer of PDMS throughout the surface of the foam films, which in turn will lead to easier formation of unstable bridges and faster foam destruction.

The exact mechanism by which the prespread layer facilitates the particle entry is still not very clear, and further experiments are planned to elucidate this point. In contrast, the destabilizing effect of the spread layer on an already formed bridge can be easily explained in the framework of the model developed in ref 18. The spread layer could supply oil to newly formed bridges, thus increasing their actual volume. As a result, bridges which were initially stable (with the initial volume being below the critical value for given contact angles and film thickness) become unstable after accumulating some additional oil.[18]

Let us note, however, that none of our observations imply that spreading (positive S or S^I) is a necessary condition for antifoam activity—neither in the bridging−stretching mechanism nor in the bridging−dewetting mechanism which was observed with another system (see below). The latter statement reinforces the conclusion of Garrett et al.[12] that spreading is not a necessary condition for antifoam activity. Note, however, that the system studied by Garrett et al.[12] was carefully chosen to avoid any spreading (even as a molecular film) of the oil, so that their arguments to reach the same conclusion were quite different from ours.

Optimal Size of the Antifoam Particles. As mentioned in the Introduction, two possibilities for destroying the foam are discussed in the literature—rupture either of the draining foam films or of the Gibbs−Plateau border.

All our experiments showed that in the studied system the foam destruction occurs mainly by rupture of the foam films. This process was directly observed in the experiments with both small horizontal films (Scheludko cell) and large vertical films. In addition, we have some indirect arguments in favor of the suggestion that mainly the planar films in particular are destroyed in real foams (in our experimental systems). As mentioned above, the average diameter (by number) of the antifoam particles

(50) Bergeron, V.; Langevin, D. *Phys. Rev. Lett.* **1996**, *76*, 3152.

in emulsion A was about 1 μm. This size corresponds well to the observed typical thickness at which the foam films in the Scheludko cell were broken. From this viewpoint the lifetime of the foam films corresponded to the period required for film thinning down to a thickness similar to the particle diameter, and in our experiments this was about 5 s. On the other hand, the foams in the Shake-Test were totally destroyed in a similar time scale (around 10 s). Therefore, it can be concluded that the time taken for foam film drainage down to the particle size was the rate-determining step in the foam destruction. In this time scale the cross-section of the Gibbs−Plateau channels is still much larger than the diameter of the particles in emulsion A. It is unlikely that the antifoam particles are able to destroy channels that are orders of magnitude larger in a cross-section. We can conclude that the foam in the Shake-Test in the presence of emulsion A was destroyed mainly by rupture of the films, just as in the model experiments with single films. Similar arguments can be used also for compound A.

The above discussion suggests that the optimal size of the antifoam particles could be estimated from the characteristic film thickness at which the rupture takes place. If the foam is to be destroyed in a period of for example 20−30 s, then particles of number average diameter d corresponding to the film thickness $\sim$ 10 s after film formation are needed. In addition, the particles should be of high enough concentration (e.g. 5−10 particles captured in a millimeter-sized foam film) and should be very active (as they were in our experiments) to destroy the film. Otherwise, the particles will escape from the film into the neighboring GPB, and the foam will remain stable at that stage. Note that it is not advisable to use particles of substantially larger diameter (than that indicated above), because the gain in bridging the film surfaces at a somewhat earlier stage could be suppressed by the strongly reduced number of antifoam particles (at the same total mass concentration m), because the number concentration $n \sim m/d^3$. On the contrary, using particles of much smaller diameter (than that estimated above) will also lead to slower destruction of the foam, because a much longer time for film thinning will be required before the particles could bridge the film surfaces.[2,10]

If the antifoam particles are not able to destroy the foam films (e.g., due to difficult entry), then the destruction of a bulk foam could start only after the water drainage results in significant narrowing of the GPBs, so that their cross-section becomes comparable to the diameter of the particles. The narrow GPB will compress the antifoam particles (drops and/or lenses) under high capillary pressure and will force them to coalesce with each other and with the air−water interface.[21] The final result of these processes will be the formation of unstable bridges in the GPB and subsequent foam destruction. Note that such a mechanism of foam rupture will require a much longer period of time (several minutes or longer) because water drainage from the GPB is a far slower process than the process of film thinning.

We do accept that in other systems (less active antifoams) the destruction of the foam occurs in the GPB, as suggested by Koczo et al.[21] This is certainly true for long-living foams (in the presence of antifoam), because our experiments indicate that the film thickness becomes smaller than the particle diameter and that the antifoam particles (if they have not already ruptured the film) are expelled into the Gibbs−Plateau borders, typically 1 min after the film is formed. In such cases, much larger particles (tens of micrometers in diameter) could be more efficient for antifoaming, because they could rupture the GPB at an earlier stage of drainage (i.e., at larger cross-section of the GPB).

Furthermore, the rate of foam-film thinning depends very much on the nature and concentration of the surfactants. Therefore, the typical time scales for film thinning with other substances (e.g., proteins or surface active synthetic polymers) could be rather different compared to that in our experiments with a low-molecular-weight surfactant. Model experiments with single foam films (like those in the Scheludko cell) can be used to monitor the film-thinning process and to determine its characteristic time scale.

Let us specify what is the characteristic size of the antifoam particles that rupture the films (drops or lenses). If we consider emulsified droplets, their characteristic size is the drop diameter. If the film destruction by lenses is considered (as it was in the experiments with compound A), then the characteristic size is the penetration depth of the lenses into the surfactant solution. As discussed in the second part of the study,[18] the penetration depth of the oil lenses depends on the three-phase contact angle air−water−oil. However, the silica particles captured in the lenses (see Figure 4B) could substantially increase the penetration depth, facilitating the bridge formation and the film rupture. In this case the penetration depth is determined mostly by the size of the silica particles.

Possible Mechanism of Antifoam Deactivation (Exhaustion). Several hypotheses were suggested in the literature to explain exhaustion of antifoams during the course of their action. Bergeron et al.[10] found that the size of the antifoam particles decreases during the foaming process. As a result, these authors argued that the foam films should drain down to smaller thickness before film bridging and rupture occur. Racz et al.[31] suggested that emulsification of the spread oil layer is the main reason for loss in antifoam efficiency. The latter possibility could be important for compounds (which are initially deposited on the solution surface), but could not be the major process in exhausting emulsified antifoams (like emulsion A), which are in the form of droplets even in the initial active period.

Our own experiments (manuscript in preparation) showed that, along with the reduction of the particle size, the antifoam deactivation is caused also by a segregation of the antifoam into two different populations of particles: silica-free and silica-enriched. Both these populations are substantially less active (due to the inappropriate silica concentration) than the initial formulation, which has an optimal silica concentration. A similar idea was suggested years ago by Pouchelon and Araud.[32]

Whatever is the mechanism of exhaustion (size reduction and/or silica−oil segregation), the question about the critical step changing the antifoam particles remains open. The mechanism of bridging−stretching discussed above suggests one possible path leading to particle size reduction and silica−oil segregation. Indeed, the process of bridge stretching and rupture is accompanied by a very rapid expansion of the oil rim (the thicker periphery of the bridge)—see Figure 12. This expansion should lead to a Rayleigh type of instability (similar to the spontaneous process of subdivision of a continuous liquid jet into droplets) and to fragmentation of the oil rim into several droplets. The size of these droplets will be smaller than the size of the initial droplet (that formed the bridge) by a factor on the order of $N^{1/3}$, where N is the number of the formed fragments. We could not see this fragmentation process in our experiments (the magnification and the time resolution are too low), but one could expect that N is a number on the order of 3−8. Furthermore, the

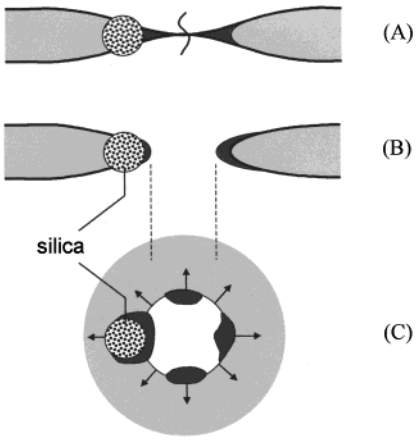

Figure 12. Possible mechanism of antifoam fragmentation. After an oil bridge ruptures (A), the formed hole in the film rapidly expands (B). The oil rim, that remained from the bridge, is stretched, which possibly leads to its fragmentation into several smaller oil droplets (C). Some of them will contain silica particles, while others could be deprived of silica. These droplets hit with high velocity the adjacent Gibbs−Plateau borders and can be emulsified there.

fragmentation process could lead to the formation of oil fragments which are free of silica (while enriching other fragments), thus inducing a process of silica−oil segregation. The oil fragments are dragged by the expanding hole in the film and are projected with very high velocity (on the order of 10 m/s) toward the Gibbs−Plateau borders. It is likely that some of the oil fragments will enter the GPB and will be trapped there in the form of small emulsion droplets (some of them containing silica). In conclusion, the drop size reduction and silica−oil segregation which are the main reasons for antifoam exhaustion in the studied system arise as a natural consequence of the bridging−stretching mechanism.

How General Are the Observed Phenomena? An overview of the literature on the mechanism of antifoam action shows that (with a few exceptions) the authors usually tend to claim generality of the mechanism which they are discussing. Our feeling is that a general, universal mechanism of antifoam action does not exist in reality. Our own preliminary experiments with a completely different experimental system (nonspreading organic oil and hydrophobized silica particles as an antifoam compound; 15 mM tetradecyltrimethylammonium bromide as a surfactant) suggest that the films in that system rupture by bridging−dewetting. Since the used substances and the arguments concerning the mechanism are very different (although the methods are similar), we will present the results from these experiments in a separate article.

In conclusion, different mechanisms, such as those shown in Figures 1 and 11, could occur in real systems, and direct methods for foam film observation (like those described above) could be applied to identify the specific mechanism in each particular case.

Conclusions

By combining several complementary experimental techniques, the mechanism of foam film destruction by a mixed (silica−silicone oil) antifoam for AOT solutions has been elucidated. When the film thickness becomes similar to the diameter of the antifoam drops (or to the penetration depth of antifoam lenses), oil bridges are formed. These bridges stretch with time, due to uncompensated capillary pressures across the oil−water and air−water interfaces,[17,18] which eventually leads to bridge perforation and foam film rupture—Figure 11.

The observations have revealed an important role of the prespread molecular layer of silicone oil (being only a few nanometers in thickness) on foam film stability. In the absence of a spread layer, most of the antifoam particles leave the foam film without making bridges. Even when bridges are formed, they are relatively stable. On the contrary, in the presence of a prespread oil layer, the particles readily make unstable bridges which rupture the foam film. Therefore, the spread oil facilitates the particle entry (by a mechanism which is not entirely clear at the present time) and destabilizes the bridges. The latter effect is explained in detail in the second part of the study.[18]

The results suggest that the observed mechanism of film rupture (bridging−stretching) is responsible for the destruction of bulk foams in the studied systems. The effects of different variables, like the values of E, S, and B, the size of the antifoam particles, and others, are discussed from this viewpoint. With other systems (antifoams, surfactants), one could expect other mechanisms to be operative (e.g., those shown in Figure 1). The combination of experimental methods for direct monitoring of the process of film rupture described above can be rather helpful to reveal the specific mechanism of foam destruction in each particular system.

Acknowledgment. The authors are indebted to Dr. V. Bergeron, Dr. M. Deruelle, Dr. Y. Giraud, and Dr. P. Branlard (Rhodia) for helpful discussions and for the continuous support of the present study. The critical reading of the manuscript by Dr. Bergeron, Dr. Deruelle, and Dr. K. Marinova (Sofia University) is gratefully acknowledged. Some of the figures were generously prepared by Dr. Marinova.

LA9902136